


# Simple and accurate model of fracture toughness of solids

Cite as: J. Appl. Phys. **125**, 065105 (2019); <https://doi.org/10.1063/1.5066311>

Submitted: 14 October 2018 . Accepted: 27 November 2018 . Published Online: 13 February 2019

Haiyang Niu, Shiwei Niu, and Artem R. Oganov 



View Online



Export Citation



CrossMark

## ARTICLES YOU MAY BE INTERESTED IN

### Frontiers of magnetic force microscopy

Journal of Applied Physics **125**, 060901 (2019); <https://doi.org/10.1063/1.5050712>

### $\Phi$ memristor: Real memristor found

Journal of Applied Physics **125**, 054504 (2019); <https://doi.org/10.1063/1.5042281>

### Modulating near-field heat transfer using oxygen-contaminated piezoelectric aluminum nitride nanomaterials

Journal of Applied Physics **125**, 065102 (2019); <https://doi.org/10.1063/1.5067244>

## Ultra High Performance SDD Detectors



# Simple and accurate model of fracture toughness of solids

Cite as: J. Appl. Phys. 125, 065105 (2019); doi: 10.1063/1.5066311

Submitted: 14 October 2018 · Accepted: 27 November 2018 ·

Published Online: 13 February 2019




View Online



Export Citation



CrossMark

Haiyang Niu,<sup>1,a)</sup> Shiwei Niu,<sup>2,3,b)</sup> and Artem R. Oganov<sup>4,5,6,c)</sup> 

## AFFILIATIONS

<sup>1</sup>Department of Geosciences and Center for Materials by Design, Institute for Advanced Computational Science, State University of New York, Stony Brook, New York 11794-2100, USA

<sup>2</sup>College of Mining and Safety Engineering, Shandong University of Science and Technology, Qingdao 266590, China

<sup>3</sup>Mining Technology Institute, Taiyuan University of Technology, Taiyuan 030024, China

<sup>4</sup>Skolkovo Institute of Science and Technology, Skolkovo Innovation Center, 4 Nobel Street, Moscow 143026, Russia

<sup>5</sup>Moscow Institute of Physics and Technology, 9 Institutsky Lane, Dolgoprudny 141700, Russia

<sup>6</sup>International Center for Materials Discovery, Northwestern Polytechnical University, Xi'an 710072, China

**Note:** This paper is part of the Special Topic on: Ultra-Hard Materials.

<sup>a)</sup>haiyang.niu@phys.chem.ethz.ch

<sup>b)</sup>nshiwei1123@gmail.com

<sup>c)</sup>a.oganov@skoltech.ru

## ABSTRACT

Fracture toughness  $K_{IC}$  plays an important role in materials design. Along with numerous experimental methods to measure the fracture toughness of materials, its understanding and theoretical prediction are very important. However, theoretical prediction of fracture toughness is challenging. By investigating the correlation between fracture toughness and the elastic properties of materials, we have constructed a fracture toughness model for covalent and ionic crystals. Furthermore, by introducing an enhancement factor, which is determined by the density of states at the Fermi level and atomic electronegativities, we have constructed a universal model of fracture toughness for covalent and ionic crystals, metals, and intermetallics. The predicted fracture toughnesses are in good agreement with experimental values for a series of materials. All the ingredients of the proposed model of fracture toughness can be obtained from first-principles calculations or from experiments, which makes it suitable for practical applications.

Published under license by AIP Publishing. <https://doi.org/10.1063/1.5066311>

## INTRODUCTION

Fracture toughness  $K_{IC}$  measures the resistance of a material against crack propagation and is one of the most important mechanical properties of materials.<sup>1</sup> For example, materials used in drilling bits or in ballistic vests should possess not only high hardness, but also high fracture toughness. The most widely used materials, diamond and tungsten carbide (WC), have drawbacks. Diamond is expensive and has problems with chemical and thermal stability, while WC is very dense (ruling out some applications) and is not super-hard. Numerous methods have been employed to experimentally measure this property. Theoretical understanding and prediction of the fracture toughness of materials have

attracted enormous attention.<sup>2-4</sup> A simple approach is to seek a correlation between cohesive energy and fracture toughness.<sup>3</sup> However, as we know, metals have much higher  $K_{IC}$ , while having lower cohesive energies than covalent and ionic crystals. Apparently,  $K_{IC}$  is not a function of just the scalar cohesive energy. By introducing more detailed mechanical and quantum-mechanical attributes of bonding,<sup>2,4</sup> such as the ideal strength, band gap, ionicity, etc., the correlation between bonding properties and fracture toughness of materials is improved but still insufficient for actual applications.

Similar to fracture toughness, measuring hardness involves fracture and deformation under mixed loading conditions. There have been several attempts to establish correlations

between hardness and one single elastic property such as bulk modulus or shear modulus.<sup>5-7</sup> By combining shear modulus and the Pugh modulus ratio  $B/G$ <sup>8</sup> ( $B$  and  $G$  refer to bulk and shear modulus, respectively), an empirical model for predicting hardness of polycrystalline material has been proposed by Chen *et al.*<sup>9</sup> and proved to be very reliable by many applications.<sup>10-13</sup> Furthermore, by introducing the concept of bond strength, other researchers have proposed robust hardness models for covalent<sup>14</sup> and ionic crystals.<sup>15</sup> By combining shear modulus and a so-called unstable stacking energy, Rice proposed the way to calculate the fracture toughness of Mode II and Mode III fracture.<sup>16</sup> These attempts inspired us to consider whether it is possible to construct a model of fracture toughness based on the elastic and electronic properties of materials.

In this work, we propose a simple and accurate model of fracture toughness for covalent and ionic crystals using mainly the elastic properties of materials. Considering that the fracture toughness of metals is usually 1-2 orders higher than that of covalent and ionic crystals, we introduce an enhancement factor by combining the density of states at the Fermi level and electronegativity of the constituent atoms. With that, we obtain a universal, simple, and physically transparent model, working across three orders of magnitude and applicable to covalent and ionic crystals, metals, and intermetallics. All the parameters in the model can be easily obtained by first-principles calculations, which makes the model applicable to materials selection and design.

## THEORETICAL BACKGROUND

Theoretical stress intensity factor to propagate a crack for materials with a crack under Mode I loading (the load is normal to the cleavage plane) can be understood through theoretical analysis.<sup>17,18</sup> Through breaking atomic bonds, a crack propagates and consequently, new surfaces are generated. The surface tension of the opening surfaces at the crack tip  $2\gamma_s$  ( $\gamma_s$  is the surface energy of the material) is the force to balance this elastic driving force. Therefore, the critical value of the stress intensity factor under Mode I loading is given by

$$K_g = 2\sqrt{\gamma_s G / (1 - \nu)}, \quad (1)$$

where  $\nu$  is Poisson's ratio and  $G$  is shear modulus. When the stress intensity factor of a crack reaches  $K_g$ , a crack propagates.  $K_g$  is the so-called theoretical fracture toughness.<sup>19</sup> In practice, an experimentally measured fracture toughness  $K_{IC}$  is considerably lower than  $K_g$ , making Eq. (1) not useful in practice. However, the underlying physical correlation between fracture toughness and the elastic properties provides useful insight.

## FRACTURE TOUGHNESS MODEL FOR COVALENT AND IONIC CRYSTALS

In order to evaluate the correlation between the shear modulus  $G$  and the experimental fracture toughness  $K_{IC}$ , we plot in Fig. 1 experimental  $K_{IC}$  against shear modulus  $G$  for a series of covalent and ionic crystals. We can see that the

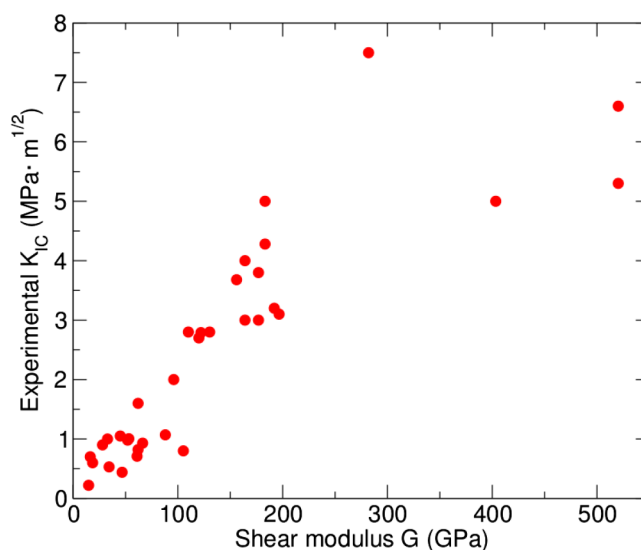


FIG. 1. Correlation between shear modulus  $G$  and experimental fracture toughness  $K_{IC}$ .

correlation between  $K_{IC}$  and  $G$  is not linear, but in general,  $K_{IC}$  increases with  $G$  with the correlation coefficient between them of 0.90. Therefore, it is promising to get a model of fracture toughness by adding some correction to the correlation between  $K_{IC}$  and  $G$ .

One possible correction factor is the well-known Pugh modulus ratio  $B/G$ .<sup>8</sup> Pugh<sup>8</sup> found that  $B/G$  is closely related with brittleness and ductility of materials. The lower the value of  $B/G$  is, the more brittle the material would be. Importantly, Pugh<sup>8</sup> also highlighted that the critical strain at fracture can be measured as  $\epsilon \propto (B/G)^2$ . During deformation of a material, bonds break and reform resulting in displacement of atoms and slipping of atomic planes, and materials with high fracture toughness usually exhibit high ductility and yield at high critical strain. Therefore, we conclude that  $B/G$  is in positive correlation with fracture toughness  $K_{IC}$ .

By combining shear modulus  $G$  and Pugh modulus ratio  $B/G$ , we propose the following empirical relation:

$$K_{IC} \propto G \cdot (B/G)^k. \quad (2)$$

In order to have correct dimensionality of  $K_{IC}$  (MPa·m<sup>1/2</sup>), a length scale unit must be added. Here, we have added volume per atom  $V_0$  to the above relation, and by fitting to the data in Table I, we can get the value of  $k$  to be about 0.5. Thus, we can obtain the following empirical formula for calculating the fracture toughness of covalent and ionic crystals:

$$K_{IC} = V_0^{1/6} \cdot G \cdot (B/G)^{1/2}, \quad (3)$$

where  $V_0$  is the volume per atom (in m<sup>3</sup>),  $G$  and  $B$  are shear and bulk moduli (in MPa), respectively, and the unit of  $K_{IC}$  is

**TABLE I.** Comparison between predicted fracture toughness  $K_{IC}$  and available experimental values at room temperature for a series of covalent and ionic crystals, along with predictions for some materials, such as  $\text{CrB}_4$ ,  $\gamma\text{-B}_{28}$ , and  $\text{Fe}_3\text{C}$ . The calculated shear modulus  $G$ , bulk modulus  $B$ , volume per atom  $V_0$ , and Pugh's modulus ratio  $B/G$  are also given. Experimental  $K_{IC}$  obtained according to American Society for Testing and Materials (ASTM) standards is taken from Ref. 20 unless otherwise specified. Experimental  $H_V^{exp}$  is taken from Refs. 9 and 14 unless otherwise specified. Predicted  $H_V^{pre}$  is estimated by Chen's model.<sup>9</sup> Elastic properties and volume per atom  $V_0$  of materials are calculated within the framework of density functional theory using the Perdew, Burke, and Ernzerhof (PBE) exchange-correlation functional<sup>21</sup> within the generalized gradient approximation and the projector-augmented waves method<sup>22</sup> as implemented in Vienna Ab Initio Simulation Package (VASP).<sup>23,24</sup> The calculated bulk ( $B$ ) and shear ( $G$ ) moduli are determined with Reuss-Voigt-Hill approximation.<sup>25</sup>

| Material                         | $G$<br>(GPa) | $B$<br>(GPa) | $V_0$<br>(Å <sup>3</sup> /atom) | $B/G$ | $K_{IC}^{exp}$<br>(MPa m <sup>1/2</sup> ) | $K_{IC}^{pre}$<br>(MPa m <sup>1/2</sup> ) | $H_V^{exp}$<br>(GPa) | $H_V^{pre}$<br>(GPa) |
|----------------------------------|--------------|--------------|---------------------------------|-------|---|---|----------------------|----------------------|
| Diamond                          | 520.3        | 431.9        | 5.70                            | 0.83  | 5.3, 6.6, 6.7                             | 6.33                                      | 96                   | 93.5                 |
| WC                               | 301.8        | 438.9        | 10.61                           | 1.46  | 7.5 (Ref. 20)                             | 5.40                                      | 24, 30               | 29.3                 |
| BN                               | 403.4        | 403.7        | 5.95                            | 1.00  | 5   | 5.43                                      | 66                   | 63.8                 |
| TiN                              | 183.2        | 282          | 9.66                            | 1.54  | 3.4, 4.28, 5.0 (Ref. 20)                  | 3.32                                      | 23                   | 22.5                 |
| TiC                              | 176.9        | 250.3        | 10.19                           | 1.42  | 2-3, 3.8 (Ref. 20)                        | 3.10                                      | 24.7                 | 24.5                 |
| SiC                              | 196.6        | 224.9        | 10.49                           | 1.14  | 3.1, 3.3, 4.0                             | 3.11                                      | 34                   | 34.5                 |
| Al <sub>2</sub> O <sub>3</sub>   | 164.3        | 254.2        | 8.75                            | 1.55  | 3 (Ref. 28), 3-4.5                        | 2.93                                      | 20                   | 20.6                 |
| B <sub>4</sub> C                 | 191.9        | 225.8        | 7.42                            | 1.18  | 3.08, 3.2, 3.7                            | 2.91                                      | 30                   | 32.8                 |
| AlN                              | 122.1        | 194.1        | 10.63                           | 1.59  | 2.79                                      | 2.28                                      | 18                   | 16.3                 |
| TiO <sub>2</sub>                 | 110.1        | 209.2        | 12.22                           | 1.90  | 2.1 (Ref. 29), 2.8                        | 2.30                                      |                      | 11.7                 |
| $\alpha\text{-Si}_3\text{N}_4$   | 120.1        | 233.8        | 10.62                           | 1.95  | 3.12 (Ref. 30)                            | 2.48                                      |                      | 12.1                 |
| MgO                              | 130.3        | 158.3        | 9.67                            | 1.21  | 1.9, 2.0                                  | 2.09                                      |                      | 24.5                 |
| ThO <sub>2</sub>                 | 88.1         | 187.7        | 14.79                           | 2.14  | 1.07                                      | 2.01                                      |                      | 8.3                  |
| MgAl <sub>2</sub> O <sub>4</sub> | 96.1         | 180.2        | 9.73                            | 1.88  | 1.83, 1.94, 1.97                          | 1.92                                      |                      | 10.8                 |
| Y <sub>2</sub> O <sub>3</sub>    | 61.3         | 138.5        | 15.33                           | 2.26  | 0.71                                      | 1.45                                      | 7.5                  | 5.5                  |
| ZnO <sub>2</sub>                 | 62.1         | 113.8        | 10.15                           | 2.32  | 1.6, 2.5                                  | 1.39                                      |                      | 5.3                  |
| Si                               | 66.3         | 98.2         | 20.41                           | 1.48  | 0.79, 0.95                                | 1.33                                      | 12                   | 11.7                 |
| GaP                              | 55.8         | 88.8         | 21.18                           | 1.59  | 0.9 (Ref. 28)                             | 1.17                                      | 9.5                  | 9.2                  |
| Ge                               | 53.1         | 72.2         | 24.17                           | 1.36  | 0.59-0.64 (Ref. 31)                       | 1.05                                      | 11.2                 | 8.8                  |
| MgF <sub>2</sub>                 | 52.2         | 95.3         | 11.36                           | 1.83  | 0.98                                      | 1.05                                      |                      | 6.9                  |
| GaAs                             | 46.7         | 75.5         | 23.92                           | 1.62  | 0.44 (Ref. 32)                            | 1.01                                      | 7.5                  | 7.8                  |
| BaTiO <sub>3</sub>               | 45.1         | 94.9         | 13.15                           | 2.11  | 1.05                                      | 1.01                                      |                      | 4.7                  |
| InP                              | 34.3         | 72.5         | 26.99                           | 2.11  | 0.42-0.53 (Ref. 34)                       | 0.86                                      | 5.4                  | 3.6                  |
| ZnS                              | 32.8         | 78.4         | 20.21                           | 2.39  | 0.75, 1.0                                 | 0.84                                      | 1.8                  | 2.5                  |
| ZnSe                             | 28.1         | 58.4         | 23.60                           | 2.07  | 0.32 (Ref. 28), 1 (Ref. 28)               | 0.68                                      | 1.4                  | 2.9                  |
| CdS                              | 18.6         | 61.1         | 26.07                           | 3.28  | 0.33-0.76 (Ref. 33)                       | 0.58                                      |                      |                      |
| CdSe                             | 16.3         | 53.1         | 29.79                           | 3.26  | 0.33-1.2 (Ref. 33)                        | 0.52                                      |                      |                      |
| NaCl                             | 14.8         | 24.9         | 22.61                           | 1.69  | 0.17-0.22 (Ref. 35)                       | 0.32                                      | 0.3                  | 2.2                  |
| WB <sub>3</sub>                  | 220.1        | 307.2        | 8.79                            | 1.40  |   | 3.73                                      | 28.1-43.3 (Ref. 27)  | 28.8                 |
| CrB <sub>4</sub>                 | 261.0        | 265.3        | 7.45                            | 1.01  |   | 3.68                                      |                      | 48                   |
| SiO <sub>2</sub> <sup>a</sup>    | 220.0        | 305.0        | 7.75                            | 1.37  |   | 3.64                                      | 33                   | 30.4                 |
| $\gamma\text{-B}_{28}$           | 236.0        | 224.0        | 6.99                            | 0.95  |   | 3.18                                      | 50                   | 49.0                 |
| B <sub>6</sub> O                 | 204.0        | 228.0        | 7.39                            | 1.12  |   | 3.01                                      | 38                   | 36.4                 |
| Fe <sub>3</sub> C                | 81.5         | 223.2        | 9.51                            | 2.74  |   | 1.96                                      |                      | 5.1                  |

<sup>a</sup>Stishovite.

in MPa m<sup>1/2</sup>. The comparison between the predicted and experimental fracture toughness is graphically represented in Fig. 2. As we can see, the predicted values are in agreement with experimental results. By calculating the correlation coefficient between predicted and experimental values, we have found this value to be 0.97. Furthermore, the root mean square error (RMSE) is estimated to be about 0.4 MPa m<sup>1/2</sup>. The high correlation coefficient and small RMSE indicate the reliability and robustness of the proposed model of fracture toughness.

## FRACTURE TOUGHNESS MODEL FOR METALS AND INTERMETALLICS

The fracture toughness of metals is usually 1-2 orders higher than that of ionic or covalent crystals, which is due to

the lower crack sensitivity of metallic bonding compared with ionic and covalent bonds. Metallic bonds can be easily broken and reformed, while ionic and covalent bonds are very hard to break, but once broken, they are very hard to reform. If we use Eq. (3) directly to calculate the fracture toughness of a metal, the resulting  $K_{IC}$  is much lower than the experimental values. Considering the intrinsic difference between ceramics and metals, we can introduce an enhancement factor  $\alpha$  to Eq. (3) and obtain the following formula for metals:

$$K_{IC} = (1 + \alpha) \cdot V_0^{1/6} \cdot G \cdot (B/G)^{1/2}. \quad (4)$$

The enhancement factor  $\alpha$  shall distinguish between covalent and ionic crystals and metals and reflect the degree of

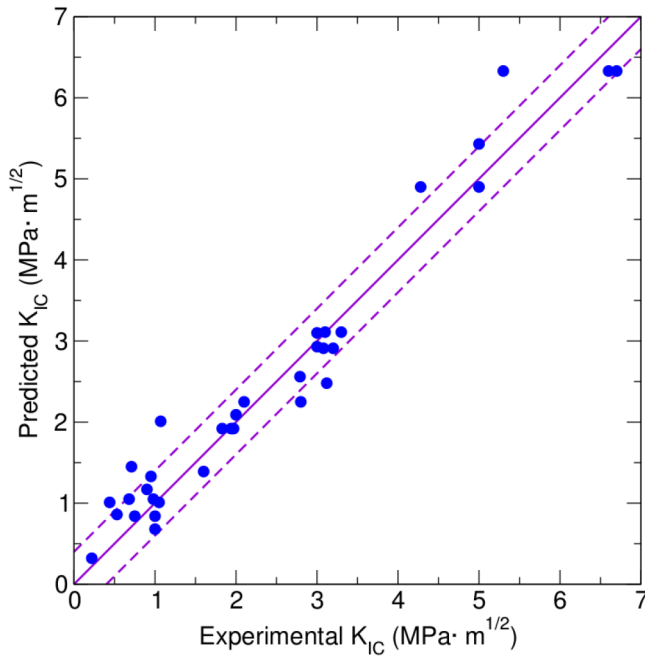


**FIG. 2.** Comparison between experimental and predicted fracture toughness  $K_{IC}$  for a series of ceramics. The root mean square error (RMSE) between experimental and predicted values is drawn with a dotted line to guide the eye.

metallicity. One choice could be the density of states (DOS) at the Fermi level. Importantly, we sum up the spin-up and spin-down electron DOS for magnetic materials to get the total DOS at the Fermi level. In order to correct the dimensionality of DOS, we need to choose a reference scale and calculate the relative DOS per volume at the Fermi level. Here, we use free electron gas as the reference. With taking aluminum's atomic volume and valence electrons, we can get the DOS at the Fermi level of the free electron gas  $g(E_F)_{FEG} = 0.025 \text{ states eV}^{-1} \text{ \AA}^{-3}$ . Thus, the relative DOS at the Fermi level  $g(E_F)_R = g(E_F)/g(E_F)_{FEG}$  of any metal can be obtained accordingly (see Table II).

By fitting the data of pure metals in Table II, we can get the form of the enhancement factor  $\alpha$  as the function of  $g(E_F)_R$

$$\alpha = 43 \cdot g(E_F)_R^{1/4}. \quad (5)$$

Different from pure metals, intermetallics are composed of two or more elements with metallic bonding. Therefore, the interaction between different elements shall be considered in the model of fracture toughness. Electronegativity is a promising factor for this purpose as it describes the tendency of an atom to attract electrons and thus forming localized states. For compound  $A_mB_n$ , we introduce an

**TABLE II.** Comparison between predicted fracture toughness  $K_{IC}$  with available experimental values at room temperature for a series of metals and intermetallics. The shear modulus  $G$ , bulk modulus  $B$ , volume per atom  $V_0$ , the enhancement factor  $\alpha$ , Pugh's modulus ratio  $B/G$ , the density of states at the Fermi level are also given. Allen scale electronegativity  $\chi^{36}$  of elements A and B of compound  $A_mB_n$  are also listed.

| Material                   | $G$<br>(GPa) | $B$<br>(GPa) | $V_0$<br>( $\text{\AA}^3/\text{atom}$ ) | $\alpha$ | $B/G$ | $g(E_F)_R$ | $\chi_A$ | $\chi_B$ | $K_{IC}^{exp}$<br>( $\text{MPa m}^{1/2}$ ) | $K_{IC}^{pre}$<br>( $\text{MPa m}^{1/2}$ ) |
|----------------------------|--------------|--------------|---|----------|-------|------------|----------|----------|--|--|
| Mg                         | 24.3         | 44.6         | 22.87                                   | 35.3     | 1.84  | 0.45       | ...      | ...      | 16-18                                      | 20.1                                       |
| Al                         | 27.6         | 75           | 16.47                                   | 44.2     | 2.72  | 1.12       | ...      | ...      | 30-35                                      | 32.8                                       |
| V                          | 37.1         | 179.2        | 13.41                                   | 65.9     | 4.84  | 5.52       | ...      | ...      | 70-150                                     | 84.0                                       |
| Ti                         | 44.8         | 110.8        | 17.05                                   | 52.3     | 2.47  | 2.18       | ...      | ...      | 50-55                                      | 60.2                                       |
| Ni                         | 82.3         | 180.8        | 10.78                                   | 68.6     | 2.20  | 6.48       | ...      | ...      | 100-150                                    | 126.2                                      |
| Fe <sup>a</sup>            | 94.1         | 193.9        | 11.97                                   | 59.2     | 2.06  | 3.60       | ...      | ...      | 120-150                                    | 123.1                                      |
| Ag                         | 29.6         | 103.8        | 17.67                                   | 36.9     | 3.51  | 0.54       | ...      | ...      | 40-105                                     | 34.1                                       |
| Au                         | 27.5         | 171.7        | 17.85                                   | 37.2     | 6.24  | 0.56       | ...      | ...      | 40-90                                      | 42.5                                       |
| $\beta$ -Sn                | 21.1         | 46.2         | 28.4                                    | 38.6     | 1.98  | 0.65       | ...      | ...      | 15-30                                      | 21.6                                       |
| Cu                         | 49.8         | 145.4        | 11.94                                   | 41.5     | 2.92  | 0.87       | ...      | ...      | 40-100                                     | 54.7                                       |
| Cu-Sn (3% Sn) <sup>b</sup> | 56.1         | 135.2        | 12.25                                   | 42.3     | 2.41  | 0.93       | ...      | ...      | 40-80 <sup>c</sup>                         | 57.1                                       |
| Cu-Sn (9% Sn) <sup>b</sup> | 47.1         | 101.1        | 12.94                                   | 39.6     | 2.15  | 0.72       | ...      | ...      | 40-80 <sup>c</sup>                         | 42.9                                       |
| Ni <sub>3</sub> Al         | 81.9         | 179.8        | 11.27                                   | 10.8     | 2.14  | 5.16       | 1.88     | 1.613    | 18.7-20.9 (Ref. 38)                        | 21.4                                       |
| FeAl                       | 95.0         | 174.9        | 11.78                                   | 8.4      | 1.84  | 4.98       | 1.80     | 1.613    | 16.6-25 (Ref. 39)                          | 18.2                                       |
| Ti <sub>3</sub> Al         | 62.6         | 115.1        | 16.51                                   | 7.2      | 1.94  | 1.08       | 1.38     | 1.613    | 14-18                                      | 11.1                                       |
| NiAl                       | 72.1         | 162.5        | 12.02                                   | 4.5      | 2.25  | 1.43       | 1.88     | 1.613    | 6.4-7.1 (Ref. 40)                          | 9.0  |
| TiAl                       | 74.8         | 109.8        | 16.15                                   | 4.9      | 1.46  | 2.26       | 1.38     | 1.613    | 8  | 8.6  |
| Al <sub>3</sub> Sc         | 65.8         | 82.1         | 17.32                                   | 3.8      | 1.24  | 0.81       | 1.613    | 1.19     | 3.5 (Ref. 41)                              | 5.8  |

<sup>a</sup>The ferromagnetic phase of Fe.

<sup>b</sup>Cu-Sn (3% Sn) and Cu-Sn(9% Sn) bronze, which are constructed by replacing 1 and 3 Cu atoms with Sn atoms in a  $2 \times 2 \times 2$  supercell of Cu FCC lattice, respectively.

<sup>c</sup>Tin bronze. Elastic properties, electronic properties, and volume per atom  $V_0$  of materials are calculated within the framework of density functional theory using the PBE exchange-correlation functional<sup>21</sup> within the generalized gradient approximation and the projector-augmented waves method<sup>22</sup> as implemented in VASP.<sup>23,24</sup> The calculated bulk ( $B$ ) and shear ( $G$ ) moduli are determined with Reuss-Voigt-Hill approximation.<sup>25</sup>

electronegativity factor as

$$f_{EN} = \beta \left/ \left[ 1 + \frac{C_m^1 C_n^1}{C_{m+n}^2} \sqrt{\left( \frac{(\chi_A - \chi_B)^2}{\chi_A \cdot \chi_B} \right)} \right]^\gamma \right., \quad (6)$$

in which  $C_m^1$ ,  $C_n^1$ , and  $C_{m+n}^2$  refer to the number of combinations and  $\chi_A$  and  $\chi_B$  refer to the Allen scale electronegativity of elements A and B, respectively. The parameters  $\beta$  and  $\gamma$  can be obtained by fitting the data on intermetallics (see Table II) to be 0.3 and 8, respectively. In the above expression, both the degree of ionicity (the squared difference of electronegativity) and the strength of bonding (product of electronegativities) are taken into consideration. Therefore, we can get the enhancement factor  $\alpha$  for pure metals and intermetallics as

$$\alpha = 43 \cdot g(E_F)_R^{1/4} \cdot f_{EN}. \quad (7)$$

We can plot the relation between the enhancement factor  $\alpha$  to the relative DOS at the Fermi level  $g(E_F)_R$  and electronegativity factor  $f_{EN}$  (see Fig. 3). The enhancement factor  $\alpha$  along the electronegativity factor axis decreases much faster than along the  $g(E_F)_R$  axis. For instance,  $g(E_F)_R$  and elastic properties of TiAl are comparable with pure metals, but its fracture toughness is much lower than that of pure metals. In this case, the electronegativity factor  $f_{EN}$  plays an important role to determine the fracture toughness of such compounds.

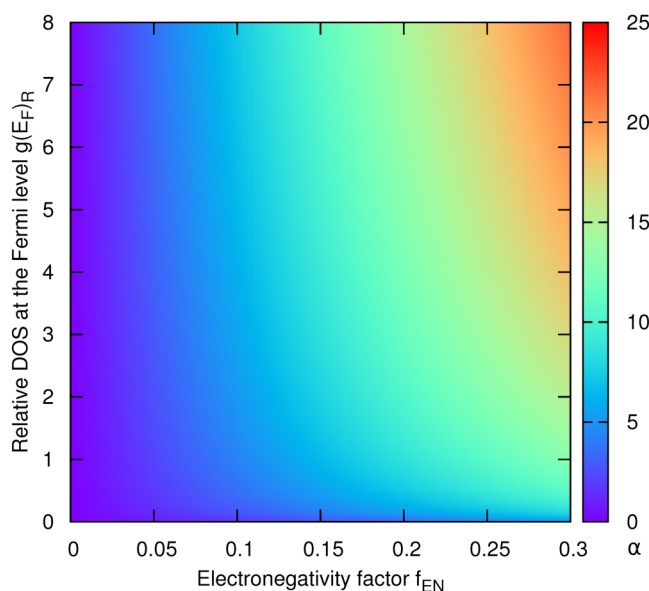


**FIG. 3.** Correlation between the enhancement factor  $\alpha$  and the electronegativity factor  $f_{EN}$  and the relative DOS at the Fermi level  $g(E_F)_R$ . The color bar gives the magnitude of the enhancement factor  $\alpha$ , which is a dimensionless factor.

## DISCUSSION

The model of fracture toughness shown in Eq. (4) is a universal model, which works for covalent and ionic crystals, metals, and intermetallics. By using Eq. (4), we have calculated fracture toughnesses for a series of metals and intermetallics as shown in Table II and plotted in Fig. 4. Experimental determination of fracture toughness can be affected by many factors. Taking into account the large spread of experimental values, our predicted results of  $K_{IC}$  are in good agreement with experimental ones. Among all the metals in Table II, we can see that the predicted and experimental fracture toughnesses of Ni and Fe are higher than those of other metals, which explains why they are intrinsically suitable for mechanical applications. From Stone Age to Bronze Age to Iron Age, technological advances and human civilization were driven by the improvement of materials. From Tables I and II, we can see that the improvement of fracture toughness played a key role in the evolution of society.

Finding materials with good comprehensive performance, such as the mechanical properties that characterize strength (e.g., hardness) and wear resistance (in particular, fracture toughness), is always the key in materials design.<sup>1</sup> With the establishment of the model of fracture toughness, we can guide the search of high performance materials through both theory and experiment. By evaluating the hardnesses of all the materials in Table I, we plot the hardness against fracture toughness of these materials (see Fig. 5).

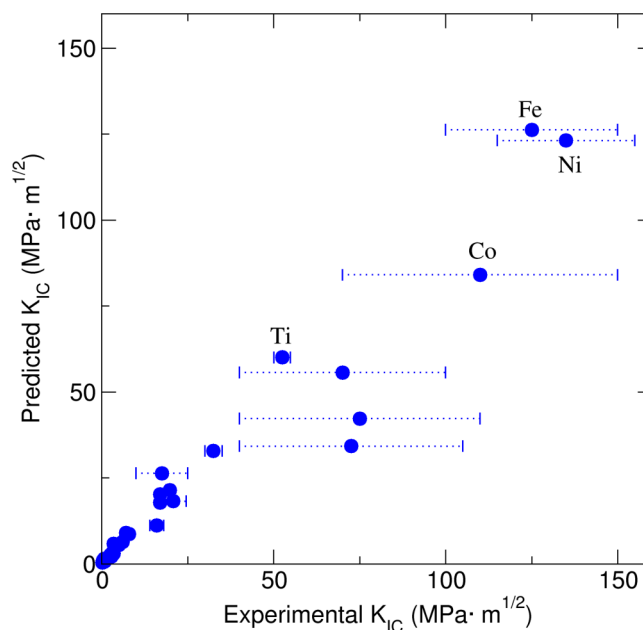


**FIG. 4.** Comparison between experimental and predicted fracture toughness  $K_{IC}$  for all the materials listed in Tables I and II. The dotted lines along the x-axis refer to the experimental  $K_{IC}$  distributions of metals.



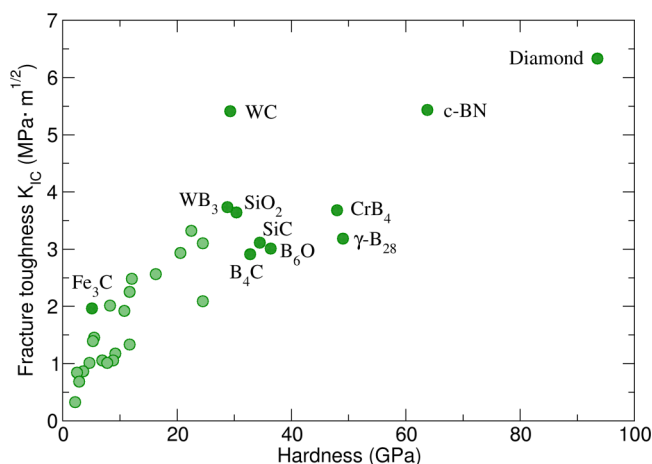


FIG. 5. Correlation between hardness  $H_v$  and fracture toughness  $K_{IC}$ .

We can see that diamond, c-BN, and WC possess the best combination of hardness and fracture toughness, which explains why they have played such an outstanding technological role. The remarkable hardness and counterintuitive high fracture toughness of diamond make it irreplaceable in many areas, such as in the mechanical processing area.<sup>26,37</sup>

## CONCLUSIONS

In this work, using the crystal structure information and properties derived from it, a simple and accurate fracture toughness model for covalent and ionic crystals has been constructed. Considering the intrinsic difference between covalent and ionic crystals and metals, we have introduced an enhancement factor  $\alpha$ , composed by the relative density of states at the Fermi level and atomic electronegativities. The relative density of states at the Fermi level can measure the degree of metallicity, while the electronegativity factor takes into account the ionicity and strength of bonding. We have demonstrated that the model of fracture toughness works for covalent and ionic crystals, metals, and intermetallics. The predicted fracture toughnesses are in good agreement with the available experimental values. It is worth noting that all the parameters in the proposed fracture toughness model can be calculated directly and accurately by first-principles calculations and can be obtained from experiment, which makes the model applicable to a wide range of practical uses.

## ACKNOWLEDGMENTS

We thank Thomas Holvey for carefully reading the manuscript. The research was supported by the Russian Science Foundation (Grant No. 17-73-20038).

## REFERENCES

- M. Ashby, *Materials Selection in Mechanical Design* (Elsevier, Amsterdam, 2004).
- Z. Ding, S. Zhou, and Y. Zhao, *Phys. Rev. B* **70**, 184117 (2004).
- S. King and G. Antonelli, *Thin Solid Films* **515**, 7232 (2007).
- S. Ogata and J. Li, *J. Appl. Phys.* **106**, 113534 (2009).
- A. Y. Liu and M. L. Cohen, *Science* **245**, 841 (1989).
- D. M. Teter, *MRS Bull.* **23**, 22 (1998).
- H. Niu, X.-Q. Chen, P. Liu, W. Xing, X. Cheng, D. Li, and Y. Li, *Sci. Rep.* **2**, 718 (2012).
- S. Pugh, *Philos. Mag.* **45**, 823 (1954).
- X.-Q. Chen, H. Niu, D. Li, and Y. Li, *Intermetallics* **19**, 1275 (2011).
- X. Zhang, Y. Wang, J. Lv, C. Zhu, Q. Li, M. Zhang, Q. Li, and Y. Ma, *J. Chem. Phys.* **138**, 114101 (2013).
- A. O. Lyakhov and A. R. Oganov, *Phys. Rev. B* **84**, 092103 (2011).
- M. Zhang, M. Lu, Y. Du, L. Gao, C. Lu, and H. Liu, *J. Chem. Phys.* **140**, 174505 (2014).
- N. G. Szwacki, *Sci. Rep.* **7**, 4082 (2017).
- F. Gao, J. He, E. Wu, S. Liu, D. Yu, D. Li, S. Zhang, and Y. Tian, *Phys. Rev. Lett.* **91**, 015502 (2003).
- A. Šimůnek and J. Vackár, *Phys. Rev. Lett.* **96**, 085501 (2006).
- J. R. Rice, *J. Mech. Phys. Solids* **40**, 239 (1992).
- A. A. Griffith and M. Eng, *Philos. Trans. R. Soc. Lond. A* **221**, 163 (1921).
- G. R. Irwin, *J. Appl. Mech.* **24**, 361 (1957).
- R. M. Thomson, *J. Phys. Chem. Solids* **48**, 965 (1987).
- R. G. Munro, S. W. Freiman, and T. L. Baker, *Fracture Toughness Data for Brittle Materials* (NIST, 1998).
- J. P. Perdew, K. Burke, and M. Ernzerhof, *Phys. Rev. Lett.* **77**, 3865 (1996).
- P. E. Blochl, *Phys. Rev. B* **50**, 17953 (1994).
- G. Kresse and J. Hafner, *Phys. Rev. B* **47**, 558 (1993).
- G. Kresse and J. Furthmüller, *Phys. Rev. B* **54**, 11169 (1996).
- R. Hill, *Proc. Phys. Soc.* **65**, 349 (1952).
- N. Cuadrado, D. Casellas Padro, L. M. Llanes Pitarch, I. Gonzalez, and J. Caro, in *Proceedings of the Euro PM2011 Powder Metallurgy Congress and Exhibition* (European Powder Metallurgy Association, 2011).
- X.-Y. Cheng, X.-Q. Chen, D.-Z. Li, and Y.-Y. Li, *Acta Cryst. C* **70**, 85 (2014).
- M. Weber, *Handbook of Optical Materials, Laser and Optical Science and Technology* (Taylor and Francis, 2002).
- G. Anstis, P. Chantikul, B. R. Lawn, and D. Marshall, *J. Am. Ceram. Soc.* **64**, 533 (1981).
- I. Tanaka, H.-J. Kleebe, M. K. Cinibulk, J. Bruley, D. R. Clarke, and M. Ruhle, *J. Am. Ceram. Soc.* **77**, 911 (1994).
- P. Lemaitre, *J. Mater. Sci. Lett.* **7**, 895 (1988).
- G. Michot, A. George, A. Chabli-Brenac, and E. Molva, *Scr. Metal.* **22**, 1043 (1988).
- M. J. Tafreshi, K. Balakrishnan, and R. Dhanasekaran, *Mater. Res. Bull.* **30**, 1387 (1995).
- F. Ericson, S. Johansson, and J.-A. Schweitz, *Mater. Sci. Eng. A* **105**, 131 (1988).
- N. Nrita, K. Higashida, and S. Kitano, *Scr. Metal.* **21**, 1273 (1987).
- L. C. Allen, *J. Am. Chem. Soc.* **111**, 9003 (1989).
- M. F. Ashby and D. Cebon, *Cambridge Engineering Selector* (CES) (Granta Design Limited, Cambridge, UK, 2013).
- J. D. Rigney and J. J. Lewandowski, *Mater. Sci. Eng. A* **149**, 143 (1992).
- P. Specht and P. Neumann, *Intermetallics* **3**, 365 (1995).
- J. Ast, B. Merle, K. Durst, and M. Goken, *J. Mater. Res.* **31**, 3786 (2016).
- W. Gerberich, S. Venkataraman, J. Hoehn, and P. Marsh, *Structural Intermetallics* (TMS, Warrendale, PA, 1993).